

# Dual multifractal spectra

Stéphane Roux<sup>(1)</sup> and Mogens H. Jensen<sup>(2)</sup>

(1): *Laboratoire Surface du Verre et Interfaces, UMR CNRS/Saint-Gobain,  
39 quai Lucien lefranc, 93303 Aubervilliers cedex, France.*

(2): *Niels Bohr Institute, Blegdamsvej 17, DK-2100 Copenhagen Ø, Denmark.*

(Dated: February 8, 2008)

The multifractal formalism characterizes the scaling properties of a physical density  $\rho$  as a function of the distance  $L$ . To each singularity  $\alpha$  of the field is attributed a fractal dimension for its support  $f(\alpha)$ . An alternative representation has been proposed by Jensen [1] considering the distribution of distances associated to a fixed mass. Computing these spectra for a multifractal Cantor set, it is shown that these two approaches are dual to each other, and that both spectra as well as the moment scaling exponents are simply related. We apply the same inversion formalism to exponents obtained for turbulent statistics in the GOY shell model and observe that the same duality relation holds here.

PACS numbers:

## I. INTRODUCTION

Initially motivated by the statistical characterization of velocity fluctuations in turbulence [2], the multifractal [3, 4] formalism has been shown to be a powerful way of analyzing a large body of different problems. It provides a simple and elegant way of performing a “dimensional analysis” of singular fields. In turbulence, this approach has been applied to the fluctuations of the velocity field, and deviation from the simple (monofractal) Kolmogorov [5] scaling of moments of different orders has been observed both experimentally [6, 7, 8, 9] and numerically [10, 11]. It has been used also to characterize the growth probabilities of Diffusion-Limited Aggregation [12]. Random resistor networks [13, 14] at the onset of percolation have also been studied using this formalism. Extension to damage and fracture models [15] have been proposed.

In those examples a local physical quantity  $m$  — referred to as a “mass” in the following for concreteness — is distributed in space (or time) and the formalism allows to characterize the statistical distribution of this quantity, or equivalently its moment of any order, as function of the system size  $L$  (or time interval) over which it is considered. The field is decomposed, according to its singularities,  $\alpha$ , into a continuous set of fractal supports. The corresponding fractal dimension  $f(\alpha)$  as a function of the singularity  $\alpha$  of the field is the multifractal spectrum. Hence, the number  $n(m)$  of elements of mass  $m$  such that

$$m \sim L^\alpha \quad (1)$$

scales as

$$n(m) \sim L^{f(\alpha)} \quad (2)$$

From this function, the scaling of any statistical moment of the field can be computed. Defining the moment of order  $q$ ,  $M_q$ , and its scaling with the system size as

$$M_q = \sum_i m_i^q \sim L^{\tau(q)} \quad (3)$$

we can relate the scaling exponents  $\tau(q)$  to the multifractal spectrum, through a simple Legendre transform [4]

$$\begin{cases} q = -f'(\alpha) \\ \tau(q) = q\alpha + f(\alpha) \end{cases} \quad (4)$$

Recently, Jensen[1] proposed to consider an alternative approach to characterize the same fields. Instead of studying the statistical distribution of mass  $m(L)$  over a fixed distance  $L$ , he proposed to consider the distribution of distances  $L(m)$  such that a fixed mass  $m$  is contained in each subset. From the initial description  $\langle m(L)^q \rangle \propto L^{\tau(q)}$  a naive expectation would have been that  $\langle L(m)^\tau(q) \rangle \propto m^q$ . However, considering the GOY model[16, 17] (as a toy-model for turbulence), it was shown that the latter expectation was violated [1]. Instead a different scaling was observed

$$\langle L(m)^p \rangle \propto m^{\theta(p)} \quad (5)$$

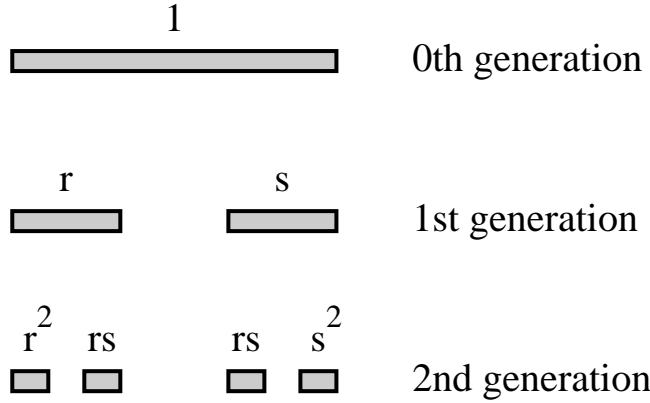


FIG. 1: Construction of the multifractal Cantor set. Starting from an interval of length  $L$  and mass  $M$  (generation 0), the first generation is obtained by splitting the interval into three equal length segments, and dropping the middle part. The mass  $M$  is distributed into two unequal parts  $rM$  and  $sM$  respectively for the left and right interval. The same procedure is repeated recursively onto each interval.

But apparently, the series of exponent  $\theta(p)$  seemed unrelated to the  $\tau(q)$ . This unexpected feature suggested to use this new scaling as a complementary statistical property of turbulence.

In the following we will consider a simple example of a multifractal set, using the standard Cantor set construction, but endowing each interval with a different mass [4]. This simple case study allows to obtain a direct evaluation of the two multifractal spectra, as well as the corresponding scaling exponents. We show that within this example both approaches are related through simple duality relations. We then discuss the applicability of the previously derived duality relations to the case of turbulence. Numerical estimates of the scaling exponents of length moments for fixed velocity differences are obtained from She and Levesque [18] proposed form for the velocity moments scaling exponents. We can apply this formula to obtain the series of exponents for the inverse statistics. To compare these “static” data to more realistic dynamical turbulence data we extract the scaling exponents for forward and inverse statistics of the GOY shell model. This was already done in [1] but here we extend the analysis to negative values of the moments of the standard forward structure functions. We then apply the inversion formula and compare to the exponents obtained by direct measurements of the inverse structure function. We obtain quite good results in the comparisons of these data sets as will be discussed in particular in Section VI. Although it is by no means a proof, it gives an indication that at least in some cases, the inversion formula we derive (which has been previously been derived in other contexts as we discuss) gives a relation between the exponents of forward and inverse statistics.

## II. STANDARD MULTISCALING FOR THE CANTOR SET

The interval of length  $L$  is split in three equal parts and the middle one is removed. The mass  $M$  is split in two unequal parts,  $rM$  and  $sM$  such that  $r + s = 1$ . After  $N$  repetitions of this procedure, we obtain a generation  $N$  structure. The size of each piece is  $\ell = 3^{-N}L$ . Its mass is  $m = r^i s^{N-i}M$ , where  $i$  is the number of  $r$  choices leading to a specific part. The number of such intervals carrying the same mass is  $n = \binom{i}{N}$ , while the total number of parts is  $S = \sum_i \binom{i}{N} = 2^N$ .

We go to the continuum limit and define the real  $x$  as  $i = xN$ . Using Stirling formula we have

$$\begin{aligned}
 n &= 2^{-N} \frac{N^N}{(Nx)^{Nx} (N(1-x))^{N(1-x)}} \\
 &= (x^x (1-x)^{(1-x)})^{-N}
 \end{aligned} \tag{6}$$

In order to bridge this computation with the standard way of defining the multifractal spectrum [4], we introduce

$$\begin{aligned}
 \alpha &= \frac{\log(m/M)}{\log(\ell/L)} \\
 f(\alpha) &= -\frac{\log(n)}{\log(\ell/L)}
 \end{aligned} \tag{7}$$

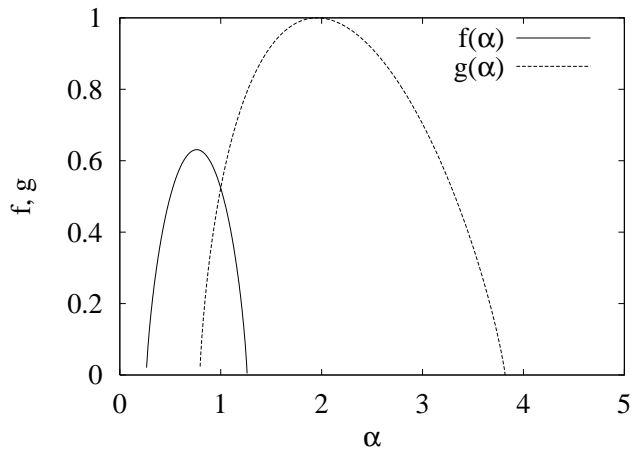


FIG. 2: Multifractal spectra for the Cantor set. The bold curve is the  $f(\alpha)$  function, while the dotted curve shows the dual spectrum  $g(\alpha)$ .

and we define  $\alpha_0 = -\log(s)/\log(3)$  and  $\alpha_1 = -\log(r)/\log(3)$ . A simple algebra leads to

$$f(\alpha) = \frac{(\alpha_1 - \alpha_0) \log(\alpha_1 - \alpha_0) - (\alpha_1 - \alpha) \log(\alpha_1 - \alpha) - (\alpha - \alpha_0) \log(\alpha - \alpha_0)}{(\alpha_1 - \alpha_0) \log(3)} \quad (8)$$

### III. MOMENT SCALING

The moment of order  $r$  of the mass distribution is defined as  $A_q(N) = \sum_i n(i)(m(i)/M)^q$ . It obeys the recursion formula

$$A_q(N) = (r^q + s^q)A_q(N-1) \quad (9)$$

For the definition of the scaling exponent  $\tau(q)$  as  $A_q(N) \propto (\ell/L)^{-\tau(q)}$  we can write

$$\tau(q) = -\frac{\log(r^q + s^q)}{\log(3)} \quad (10)$$

One basic property of the multifractal formalism is that the scaling exponents  $\tau(q)$  can be related to the multifractal spectrum through a Legendre transform. Indeed, the moment can be evaluated as  $A_q(N) = \sum_\alpha (\ell/L)^{f(\alpha)+q\alpha}$ . Hence,  $\tau(q) = \max_\alpha [f(\alpha) + q\alpha]$ . This defines the strength of the singularity  $\alpha$  which contributes dominantly to the moment of order  $q$ .

$$\begin{cases} q &= -f'(\alpha) \\ \tau(q) &= f(\alpha) + q\alpha \end{cases} \quad (11)$$

The symmetry property of the Legendre transform allows to express the reverse transformation as

$$\begin{cases} \alpha &= \tau'(q) \\ f(\alpha) &= \tau(q) - q\alpha \end{cases} \quad (12)$$

### IV. CONSTANT MASS ENSEMBLE

Now we introduce the alternative approach of truncating the hierarchical construction at a fixed mass and not fixed generation (or length). The mass  $m/M$  is chosen, and thus  $i$  and  $j$  are related by

$$r^i s^j = m/M \quad (13)$$

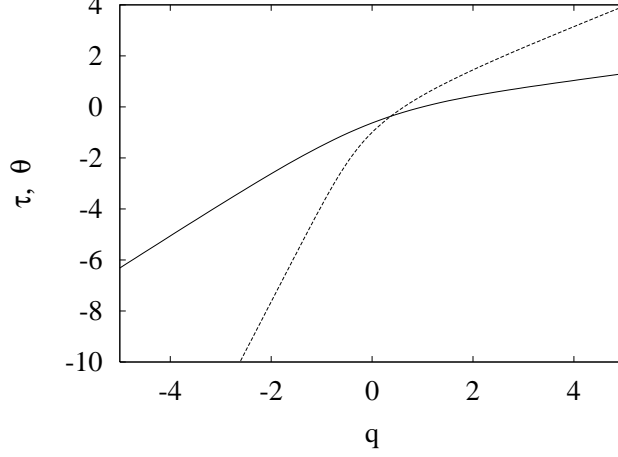


FIG. 3: Scaling exponents  $\tau(q)$  for the mass as a function of the interval length in bold line, and the dual scaling exponent  $\theta(q)$  in dotted line.

The length of such intervals is

$$\frac{\ell}{L} = 3^{-(i+j)} \quad (14)$$

and their number is  $n = \binom{i}{i+j}$ .

To mimick a similar construction as previously we define  $\ell/L = (m/M)^\beta$ , and  $n = (m/M)^{g(\beta)}$ . A simple computation leads to

$$g(\beta) = \frac{\beta(\alpha_1 - \alpha_0) \log(\beta) + \beta(\alpha_1 - \alpha_0) \log(\alpha_1 - \alpha_0) - (1 - \beta\alpha_0) \log(1 - \beta\alpha_0) - (\beta\alpha_1 - 1) \log(\beta\alpha_1 - 1)}{(\alpha_1 - \alpha_0) \log(3)} \quad (15)$$

Comparison with the original multifractal spectrum shows that they are related through

$$g(\beta) = \beta f(1/\beta) \quad (16)$$

In fact this key relation can be simply derived by noting that

$$\begin{aligned} n &= (\ell/L)^{f(\alpha)} \\ &= (m/M)^{f(\log(m/M)/\log(\ell/L)) \log(\ell/L)/\log(m/M)} \\ &= (m/M)^{\beta f(1/\beta)} \\ &= (m/M)^{g(\beta)} \end{aligned} \quad (17)$$

from which Eq.16 results.

## V. MOMENT SCALING

We introduce similar moments in the dual ensemble  $B_p = \sum n(\ell/L)(\ell/L)^p$  and define their scaling exponents  $\theta(p)$  as  $B_p \propto (m/M)^{\theta(p)}$ . As for the primal ensemble, the scaling exponents  $\theta(p)$  are related to the multifractal spectrum  $g(\beta)$  through a Legendre transform

$$\begin{cases} p &= -g'(\beta) \\ \theta(p) &= g(\beta) + p\beta \end{cases} \quad (18)$$

and reciprocally

$$\begin{cases} \beta &= \theta'(p) \\ g(\beta) &= \theta(p) - p\beta \end{cases} \quad (19)$$

Let us now use the duality relation 16 to relate the two series of scaling exponents.

$$\begin{aligned}
p &= -g'(\beta) \\
&= -f(1/\beta) + f'(1/\beta)/\beta \\
&= -f(\alpha) + f'(\alpha)\alpha \\
&= -\tau(q) + r\alpha - q\alpha \\
&= -\tau(q)
\end{aligned} \tag{20}$$

and

$$\begin{aligned}
\theta(p) &= g(\beta) + p\beta \\
&= (f(\alpha) + p)/\alpha \\
&= (\tau(q) - q\alpha - \tau(q))/\alpha \\
&= -q
\end{aligned} \tag{21}$$

Thus the two functions  $\tau$  and  $\theta$  are related by a mere inversion up to sign reversals (see also [27]),

$$-\theta(-\tau(q)) = q \tag{22}$$

One can also visualize the above result by noting that the graph of  $\theta(p)$  is obtained from that of  $\tau(q)$  through a simple symmetry with respect to the line passing through the origin and of direction  $(-1, 1)$ .

Therefore, contrary to what was initially proposed, the two series of exponents are not independent. They are linked by a duality relation, as the two multifractal spectra  $f$  and  $g$ .

## VI. APPLICATION TO TURBULENCE STATISTICS

In order to test the relevance of the above analysis to a more physical application than the Cantor set, we resort to the framework of turbulence which was the initial context of the suggestion of these dual quantities. In this context, the local physical quantity of interest is the velocity fluctuation  $\Delta u$  (instead of the mass in the above example) studied over a distance  $r$  which plays the role of the local scale  $\ell$ . The early suggestion by Kolmogorov of the scaling moments  $\tau(q) = q/3$  was shown to break down due to intermittency thus defining a non-trivial series  $\tau(q)$  which has resisted all theoretical attempts to compute them up to now. Nevertheless, semi-empirical formulas have been proposed which accounts rather precisely for the numerical values of these exponents as determined experimentally. In particular, the She and Levesque [18] formula appears as an accurate fit. They proposed

$$\tau(q) = q/9 + 2 \left( 1 - (2/3)^{q/3} \right) \tag{23}$$

Table I gives the corresponding  $\tau$  exponents for selected positive moments. In order to extract the corresponding  $\theta$  exponents for the dual statistics, we apply the inversion formula (22). Indeed, we then need to employ the She-Levesque formula for negative moments. From the derivation of this formula, it is not obvious that such extension is allowed by the assumptions made by She and Levesque. Nevertheless, we take the liberty to continue the formula to negative moments and obtain the list of exponents  $\theta$  listed in Table I.

In order to compare these results with data obtained from numerical simulations of turbulence models, and even more importantly to test the inversion formula (22), we turn to dynamical turbulence generations by shell models [10]. This kind of data were already applied in the paper by one of us which proposed the inverse structure functions [1]. In turbulence theory, it is well known that scaling behavior of velocity field  $\mathbf{u}(\mathbf{x}, t)$  and the understanding of intermittency effects in fully developed turbulence is described in terms of standard structure functions defined as

$$\langle \Delta u_{\mathbf{x}}(\ell)^q \rangle \sim \ell^{\tau_q} \tag{24}$$

where the difference is

$$\Delta u_{\mathbf{x}}(\ell) = \mathbf{u}(\mathbf{x} + \mathbf{r}) - \mathbf{u}(\mathbf{x}) \quad , \quad \ell = |\mathbf{r}| \tag{25}$$

The average in Eq.(24) is over space and time. We have assumed full isotropy of the velocity field. The set of exponents  $\tau_q$  forms a multiscaling spectrum [19].

The corresponding dual structure functions is defined by considering the following quantities

$$\langle \ell (\Delta u_{\mathbf{x}})^q \rangle \sim |\Delta u_{\mathbf{x}}|^{\theta_q} \tag{26}$$

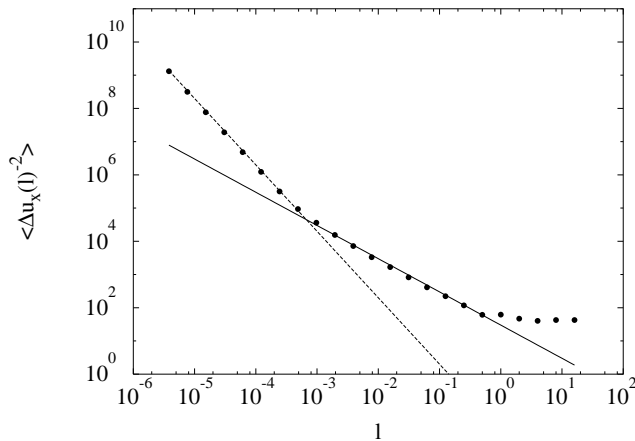


FIG. 4: A plot of the ordinary structure function from shell model data with moment  $q = -2$ , i.e.  $\langle (\Delta u_{\mathbf{x}}(\ell))^q \rangle$  versus the length scale  $\ell$ . Note the three different regimes: The small scale regime of the smooth behavior; the inertial scaling regime and outer cut-off.

where the difference  $\Delta u_{\mathbf{x}}$  is again defined as in Eq. (25) and  $\ell(\Delta u_{\mathbf{x}})$  is understood as the *minimal* distance in  $\mathbf{r}$ , measured from  $\mathbf{x}$ , for which the velocity difference exceeds the value  $\Delta u_{\mathbf{x}}$  [1]. In other words, we fix a certain set of values of the velocity difference  $\Delta u_{\mathbf{x}}$ . Starting out from the point  $\mathbf{x}$ , we monitor the distances  $\ell(\Delta u_{\mathbf{x}})$  where the velocity differences are equal to the prescribed values. Performing an average over space and time the inverted structure functions Eq. (26) are obtained.

The turbulence data are obtained from simulations of the GOY shell model [10, 16, 17]. This model is a rough approximation to the Navier-Stokes equations and is formulated on a discrete set of  $k$ -values,  $k_n = r^n$ . We use the standard value  $r = 2$ . In term of a complex Fourier mode,  $u_n$ , of the velocity field the model reads

$$\left(\frac{d}{dt} + \nu k_n^2\right) u_n = i k_n (a_n u_{n+1}^* u_{n+2}^* + \frac{b_n}{2} u_{n-1}^* u_{n+1}^* + \frac{c_n}{4} u_{n-1}^* u_{n-2}^*) + f \delta_{n,4}, \quad (27)$$

with boundary conditions  $b_1 = b_N = c_1 = c_2 = a_{N-1} = a_N = 0$ .  $f$  is an external, constant forcing, here on the forth mode. The coefficients of the non-linear terms must follow the relation  $a_n + b_{n+1} + c_{n+2} = 0$  in order to satisfy the conservation of energy,  $E = \sum_n |u_n|^2$ , when  $f = \nu = 0$ . The constraints still leave a free parameter  $\epsilon$  so that one can set  $a_n = 1$ ,  $b_{n+1} = -\epsilon$ ,  $c_{n+2} = -(1 - \epsilon)$  [20]. As observed in [21], one obtains the canonical value  $\epsilon = 1/2$ , if helicity conservation is also demanded. The set (27) of  $N$  coupled ordinary differential equations can be numerically integrated by standard techniques. We have used standard parameters in this paper  $N = 27$ ,  $\nu = 10^{-9}$ ,  $k_0 = 0.05$ , and  $f = 5 \cdot 10^{-3}$ .

The structure functions exponents  $\tau_q$  are shown in Fig. 5 for integer moments in the interval  $q \in [-10; 12]$ . A line connects the points in order to guide the eye. The associated exponents  $\theta(q)$  for the inverse structure functions are also shown in Fig. 5 for moments in the interval  $q \in [0; 12]$ , and are connected by a dotted line. It is possible to extract the exponents  $\tau_q$  to reasonable accuracy for negative moments  $-q$  although the quality of the scaling gradually decreases with the value of  $q$ . As an example we show in Fig. 4 the behavior of  $\langle \ell(\Delta u_{\mathbf{x}})^{-2} \rangle$ , corresponding to  $q = -2$ . We observe three distinct regimes: the small scales referring to the trivial smooth regime, the “inertial” scaling regime and the cut-off regime at large scales. For increasing value of negative moments, the point where  $\langle \ell(\Delta u_{\mathbf{x}})^q \rangle$  are small will be enhanced. This is a very important point to be considered for the analysis of experimental data. Indeed, the lower cut-off of the inertial, increasing with large negative values of  $q$  [22], may render the analysis of experimental data quite difficult. Using an extended self-similarity procedure (studying one moment against another one rather than as a function of the velocity difference) seem to provide better results for the inverse exponents, but since the cut-off effect is physical and not a measurement artifact, the exploitation of the data may lead to apparent contradictions [23].

It is to be noted that from duality, we may convert dual positive order moment to direct negative order moment. The latter may be very difficult to estimate experimentally because of the possible occurrence of arbitrarily small velocity differences over a given distance (or time using Taylor’s hypothesis). Therefore, the duality relation may be exploited to obtain data which would be inaccessible otherwise. This procedure however relies on the applicability of this duality to experimental turbulence, which could not be tested directly if the direct moments cannot be computed.

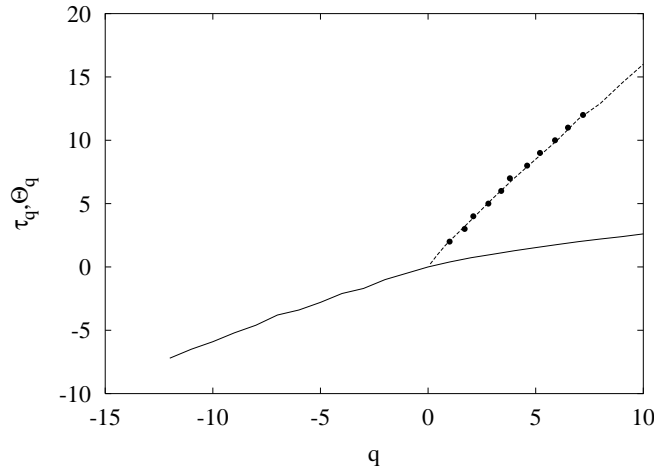


FIG. 5: Scaling exponents obtained from simulations of the GOY shell model. The full curve gives the forward structure function exponents,  $\tau_q$ . The dashed line connects the exponents  $\theta_q$  for the inverted structure functions. The black dots are the results obtained by applying the inversion formula Eq. 22 and thus transferring the data for negative  $q$ 's of  $\tau_q$  to positive  $q$ 's for  $\theta_q$ .

Nevertheless the present test of the analysis, using the shell model, constitutes an encouraging argument to proceed in this direction.

Armed with these data sets we are ready to check the validity of the inversion formula (22) which by a simple inversion reads

$$-\tau(q) = \theta^{-1}(-q) \quad (28)$$

Using the relation (22) directly by inserting  $\tau(q)$  for  $q \in [-10; -1]$  we obtain by linear extrapolation the data for  $\theta_q$  shown in Table II. The results are also shown as black dots in Fig. 5. Using the inverted relation (28), we can compare the value of  $-\tau_q$  with the values of  $\theta^{-1}(-q)$ , and these are also listed in Table II. Indeed, there is a very good correspondence between the values supporting the suggestion that the inversion formula is valid for the shell model turbulence data. This might be somewhat surprising as we do indeed perform a very different statistics.

An inversion formula similar to the one derived in this paper has been proposed for the turbulence spectra [24] and has been applied to multiaffine fields in [25]. Recently, the inverse statistics has been applied to two-dimensional turbulence with the very interesting result that the inverse statistics of a smooth signal shows non-trivial behavior [26]. Hastings has also derived a similar formula for Laplacian random walks in the very different context of diffusion limited aggregation [27]. By using iterated conformal mappings Hastings obtain the exact multifractal spectra of the harmonic measure and derive the inversion formula for the  $f(\alpha)$  spectrum.

One might express a general worry that in the integrals for the statistical averages one integrates over the same singularity structure, both to obtain the standard and inverse (i.e. dual) structure functions. That is to say that dominating terms of the integrals (and thus the saddle point) come from the same singular structures even though one might argue that for turbulence, the velocity singularities are important for the forward structure functions whereas the laminar regions are important for the dual structure functions. However, as mentioned earlier, besides the intrinsic limitations due to the evolution of the cross-over length scale between laminar and inertial regimes with the moment order, when both tools are used to analyze the inertial regime, we are characterizing the same multifractal object for which the correspondence is expected to hold. Indeed the shell model used to validate the procedure is not deprived of such singularities (looking like shock waves in that case).

## VII. CONCLUSIONS

The alternative approach to the standard multifractal spectrum and scaling exponents of different moment orders, which was proposed by interchanging the role of the physical quantity of interest and the length (or time) scale, has been examined in the case of a simple multifractal Cantor set. This example shows that the two spectra are simply related, and that the scaling exponents of the length moments can be related to the usual series of scaling exponents.

Based on this correspondence, we tested the application of this alternative approach to turbulence using data obtained from shell model calculations. A good agreement was found, thus suggesting that the above duality relation could be extended to more general cases.

### Acknowledgments

We wish to acknowledge fruitful discussions and exchanges with Massimo Vergassola and Willem van der Water.

- 
- [1] M. H. Jensen, Phys. Rev. Lett., **83**, 76 (1999).
  - [2] U. Frisch, “Turbulence: The legacy of A.N. Kolmogorov”, Cambridge University Press (1995).
  - [3] R. Benzi, G. Paladin, G. Parisi and A. Vulpiani, J. Phys. A **17**, 3521 (1984).
  - [4] T.C. Halsey, M.H. Jensen, L.P. Kadanoff, I. Procaccia, and B. Shraiman, Phys.Rev.A **33**, 1141 (1986).
  - [5] A.N. Kolmogorov, C.R. Acad. Sci. USSR **30**, 301; *ibid* **32**, 16 (1941).
  - [6] F. Anselmet, Y. Gagne, E.J. Hopfinger and R.A. Antonia, J. Fluid Mech. **140**, 63 (1984).
  - [7] C.M. Meneveau and K.R. Sreenivasan, Nucl. Phys. B Proc. Suppl.2 **49** (1987); C.M. Meneveau and K.R. Sreenivasan, P. Kailasnath and M.S. Fan, Phys. Rev. **A41**, 894 (1990).
  - [8] J. Maurer, P. Tabeling and G. Zocchi, Europhys. Lett. **26**, 31 (1994).
  - [9] J. Herweijer and W. van de Water, Phys. Rev. Lett. **74**, 4653 (1995).
  - [10] M.H. Jensen, G. Paladin and A. Vulpiani, Phys.Rev.A **43**, 798 (1991).
  - [11] T. Gotoh and D. Fukayama, Phys.Rev.Lett **86**, 3775 (2001); T. Gotoh, Comp. Phys. Comm. **147**, 530 (2002).
  - [12] P. Meakin, in Phase Transition and Critical Phenomena, vol.12, C. Domb and J.L. Leibowitz eds., Academic Press (1988)
  - [13] L. de Arcangelis, S. Redner and A. Coniglio, Phys. Rev. B. **31**, 4725 (1985).
  - [14] G.G. Batrouni, A. Hansen and M. Nelkin, J. Physique (Paris), **48**, 771, (1987)
  - [15] L. de Arcangelis and H.J. Herrmann, Phys. Rev. B **39**, 2678, (1989)
  - [16] E. B. Gledzer, Sov. Phys. Dokl. **18**, 216 (1973).
  - [17] M. Yamada and K. Ohkitani, J. Phys. Soc. Japan **56**, 4210(1987); Prog. Theor. Phys. **79**,1265(1988).
  - [18] Z.S. She and E. Levesque, Phys. Rev. Lett. **72**, 336 (1994).
  - [19] G. Paladin and A. Vulpiani, Phys. Rep. **156**, 147 (1987).
  - [20] L. Biferale, A. Lambert, R. Lima, and G. Paladin, Physica D **80**, 105 (1995).
  - [21] L. Kadanoff, D. Lohse, J. Wang, and R. Benzi, Phys. Fluids **7**, 617 (1995).
  - [22] U. Frisch and M. Vergassola, Europhys. Lett. **14**, 439 (1991).
  - [23] W. v.d. Water, private communication (2003).
  - [24] M. Vergassola, unpublished (1999).
  - [25] L. Biferale, M. Cencini, D. Vergni, and A. Vulpiani, Phys. Rev. E **60**, R6295 (1999).
  - [26] L. Biferale, M. Cencini, A. Lanotte, D. Vergni, and A. Vulpiani Phys. Rev. Lett. **87**, 124501 (2001).
  - [27] M.B. Hastings, Phys. Rev. Lett., **88**, 055506 (2002).



TABLE I: Value of some  $\tau(q)$  and  $\theta(q)$  exponents for moments of order  $q$  based on numerical simulations of the GOY shell model [10, 16, 17]. These data are as presented in Ref. [1]. For comparison, we present the corresponding series of exponents based on She and Levesque formula (index  $SL$ ). To obtain the series of the inverse exponents  $\theta_{SL}(q)$  we have invoked the inversion formula (22).

$q$	$\tau_{GOY}(q)$	$\theta_{GOY}(q)$	$\tau_{SL}(q)$	$\theta_{SL}(q)$
0.	0.00	0.00	0.000	0.00
0.2	0.08	0.45	0.076	0.51
0.4	0.15	0.89	0.150	1.00
0.6	0.22	1.3	0.222	1.46
0.8	0.29	1.7	0.294	1.91
1.	0.39	2.04	0.364	2.33
2.	0.73	3.7	0.696	4.21
3.	1.00	5.4	1.00	5.77
4.	1.28	7.0	1.28	7.09
5.	1.53	8.5	1.54	8.23
6.	1.77	10.0	1.78	9.24
7.	2.00	11.7	2.00	10.14
8.	2.20	12.9	2.21	10.95
9.	2.39	14.5	2.41	11.68
10.	2.61	16.0	2.59	12.36

TABLE II: Value of exponents obtained from simulations of the GOY model for negative moments in the interval  $q \in [-12; -2]$ . Shown are the values of  $-\tau(q)$  which according to the inversion formula should be compared to  $\theta^{-1}(-q)$ . Last row are values of  $\theta(-\tau(q))$  which should be compared to  $-q$ .

$q$	$-\tau(q)$	$\theta^{-1}(-q)$	$\theta(-\tau(q))$
-2	1.0	0.98	2.04
-3	1.7	1.59	3.1
-4	2.1	2.17	3.9
-5	2.8	2.76	5.06
-6	3.4	3.38	6.04
-7	3.8	4.0	6.7
-8	4.6	4.66	7.9
-9	5.2	5.34	8.8
-10	5.9	6.0	9.85
-11	6.5	6.59	10.85
-12	7.2	7.25	11.9